All-optical switching characteristics in bacteriorhodopsin and its applications in integrated optics

Yuhua Huang,[1,2] Shin-Tson Wu[1] and Youyuan Zhao[3]

[1]*School of Optics/CREOL, University of Central Florida, Orlando, Florida 32816, USA*
[2]*Department of Physics, East China Normal University, Shanghai, 200062, China*
[3]*Department of Optics & Engineering, Fudan University, Shanghai, 200433, China*
swu@mail.ucf.edu

http:/lcd.creol.ucf.edu

Abstract: We experimentally and theoretically investigated the optical switching characteristics of bacteriorhodopsin (bR) at λ=633 nm using the pump-probe method. A diode-pumped second harmonic YAG laser (λ=532 nm which is located around the maximum initial Br state absorption) was used as a pumping beam and a cw He-Ne laser (λ=633 nm which is around the peaks of K and O states) was used as a probe. Due to the nonlinear intensity induced excited state absorption of the K, L, M, N, and O states in the bR photocycle, the switching characteristics are sensitive to the intensity of the probe and pump beams. Based on this property, we have demonstrated an all-optical device functioning as 11 kinds of variable binary all-optical logic gates.

OCIS codes: (160.4890) Organic materials; (190.4390) Nonlinear optics, integrated optics (200.4660) Optical logic; (230.1150) All-optical device

References and links

1. H. Chun, W. J. Joo, N. J. Kim, I. K. Moon, N. Kim , "Applications of polymeric photorefractive material to reversible data storage and information processing," J. Appl. Poly. Sci. **89,** 368-372 (2003).
2. J. A. Stuart, D. L. Mercy, K. J. Wise, "Volumetric optical memory based on bacteriorhodopsin," R. R. Birge, Synth. Metals **127,** 3-15 (2002)
3. S. Roy, C. P. Singh, K. P. J. Peddy, "Analysis of spatial light modulation characteristics of C_{60}," Appl. Phys. Lett. **77,** 2656-2658 (2000).
4. K. Clays, S. V. Elshocht, and A. Persoons, "Bacteriorhodopsin: a natural nonlinear photonic bandgap material," Opt. Lett. **25,** 1391-1393 (2000).
5. P. Bhattacharya, J. Xu, G. Váró, D. L. Marcy and R. R. Birge, "Monolithically integrated bacteriorhodopsin Ga-As field-effect transistor photoreceiver," Opt. Lett. **27** 839-841 (2002).
6. D. Oesterhelt and W. Stoeckenius, Nature (London) **233,** (1971) 149
7. R. R. Birge, "Photophysics of light transduction in rhodopsin and bacteriorhodopsin," Annul Rev. Biophy. Bioeng., **10,** 315-354 (1981).
8. Q. W. Song, C. P. Zhang, R. Gross, R. Birge, "Optical limiting by chemically enhanced bacteriorhodopsin films," Opt. Lett. **18,** 775-777 (1993).
9. F. J. Aranda, R. Garimella, N. F. McCarthy, D. Narayana Rao, D. V. G. L. N. Rao, Z. Chen, J. A. Akkara, D. L. Kaplan, and J. F. Roach, "All-optical light modulation in bacteriorhodopsin films," Appl. Phys. Lett. **67,** 599-601 (1995).
10. P. Ormos, L. Fábián, L. Oroszi, E. K .Wolff, J. J. Ramsden, and A. Dér, "Protein-based integrated optical switching and modulation," Appl. Phys. Lett. **80,** 4060-4062 (2002).
11. J. Joseph, F. J. Aranda, D. V. G. L. N. Rao, B. S. DeCristofano, B. R. Kimball, and M. Nakashima, "Optical implementation of the wavelet transform by using a bacteriorhodopsin film as an optically addressed spatial light modulator," Appl. Phys. Lett. **73,** 1484-1486 (1998).

#3422 - $15.00 US Received 2 December 2003; revised 26 February 2004; accepted 28 February 2004

12. Y. H. Zhang, Q. W. Song, C. Tseronis, R. R. Birge, "Real-time holographic imaging with a bacteriorhodopsin film," Opt. Lett., **20,** 2429-2431 (1995).
13. D. V. G. L. N. Rao, F. J. Aranda, D. N. Rao, Z. Chen, J. A. Akkara, D. L. Kaplan, M. Nakashima, "All-optical logic gates with bacteriorhodopsin films,"Opt. Commun. **127**, 193-199 (1996).
14. T. Zhang, C. Zhang, G. Fu, G. Zhang, Y. Li, Q. W. Song, B. Parsons, R. R. Birge," All-optical logic gates using bacteriorhodopsin films," Opt. Eng. **39,** 527-534 (2000).
15. L. Q. Gu, C. P. Zhang, A. F. Niu, J. Li, G. Y. Zhang, Y. M. Wang, M. R. Tong, J. L. Pan, Q. W. Song, B. Parsons and R. R. Birge, "Bacteriorhodopsin based photonic logic gate and its applications to grey level image subtraction," Opt. Commun. **131,** 25-30 (1996).
16. C. P. Singh and S. Roy, "All-optical switching in bacteriorhodopsin based on M state dynamics and its application to photonic logic gates," Opt. Commun. **218,** 55-66 (2003)

1. Introduction

All-optical molecular devices have been extensively investigated for photonic applications such as large capacity information processing and storage due to their compact size and light weight [1-3]. The photochromic protein bacteriorhodopsin (bR) is one of the most promising candidates for potential applications in biomolecular photonics because of its unique properties, such as large optical nonlinearity and good stability towards photodegradation and temperature [4,5].

Bacteriorhodopsin is a light-harvesting protein found in the purple membrane of halobacterium halobium [6]. Without illumination, bR is in its initial Br state exhibiting an absorption peak at λ~570 nm. Upon absorbing photons at λ~ 570 nm, bR molecules promptly produce isomerization from all-trans to 13-cis followed by several structural transformations corresponding to the intermediate states in a complex photocycle. It has been commonly accepted that after illumination, the molecule in the initial Br state is pumped to J state and then thermally relaxes through K, L, M, N and O intermediate states back to the initial Br state, as shown in Fig. 1 [7]. With the formation of each intermediate state, the absorption spectrum produces obvious shifts, especially the absorption spectrum of the M intermediate state, which significantly shifts ~160 nm toward blue with respect to the initial Br state spectrum. Since M is the most stable intermediate state, bR can be viewed as exhibiting a bistability between the Br and M states. Various applications have been proposed based on this bistability, including optical limiting [8], optical switching [9,10], spatial light modulator (SLM) [11], optical image processing [12], and all-optical logic gate, etc [13-16].

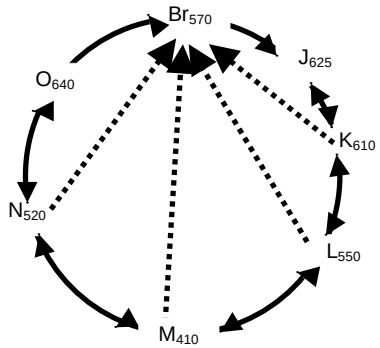

Fig. 1. Major photocycle of the bR molecules.

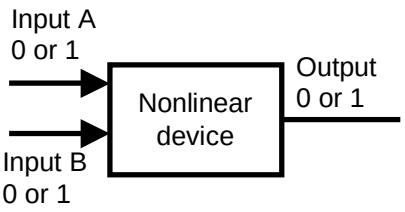

Fig. 2. The operating principles of a double binary variable logic gate.

In general, a logic gate is a logic device with two binary inputs A and B (either 0 or 1) and its output is also 0 or 1. The values 0 and 1 represent low and high intensity, respectively. Logic gates are usually achieved through a nonlinear device, as shown in Fig. 2. The output is

#3422 - $15.00 US Received 2 December 2003; revised 26 February 2004; accepted 28 February 2004

the logic result, determined by the two inputs and the nonlinear functional device. By choosing a suitable nonlinear functional device, different logic operations can be achieved.

Various types of logic gates using bR film have been proposed. For instance, an AND logic gate has been realized using sequential photo-excitation [13], and the AND and OR logic gates have been implemented in a single bR film by the degenerate four wave mixing technique [14]. Other all-optical logic gates have been designed with a single bR film based on complementary suppression-modulated transmission (CSMT) [15, 16]. Most of the previous proposals are based on the simplified Br and M two-state model. However, bR photocycle is a complex process. In some situations the contributions of K, L, N and O intermediate states cannot be neglected. These processes may result in interesting phenomena.

In this paper, we report the optical switching of bR at λ=633 nm using the pump-probe method. Due to the nonlinear effect induced excited state absorption of the K, L, M, N and O states in the bR's photocycle, the switching characteristics are sensitive to the intensity of the probe and pump beams. Based on these properties, we demonstrated an all-optical switching device which enables 11 kinds of logic operations. Our design is simple while exhibiting various logic operations in a single device. The logic operation is achieved by adjusting the probe and pump beams intensities. This approach is particularly useful for integrated optics.

2. Experiment and results

Figure 3 shows the experimental arrangement for studying the optical switching behavior using a bR film. A He-Ne laser with λ=633 nm was used as the probing beam and a diode-pumped Nd-YAG laser with ~ 1.5 mm diameter at λ=532 nm was used as the pumping beam. The probe beam was focused by lens 1 onto the sample whose diameter is ~ 28 μm. The pump and probe beams overlap on the bR film. In our experiment, the bR film was purchased from Munich Innovative Biomaterials GmbH. Its thickness is ~80 μm and optical density is 3 at λ=570 nm. The lifetime of the M intermediate state is ~5 s.

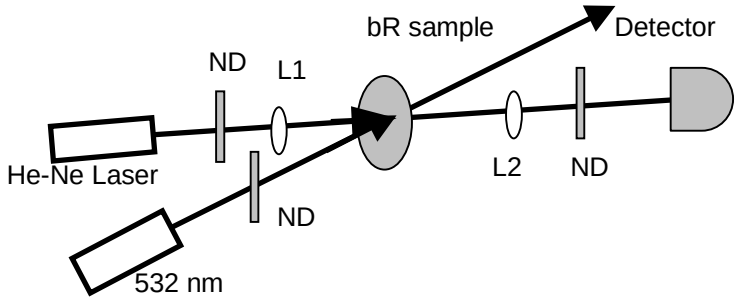

Fig. 3. Experimental setup for studying the optical switching characteristics of bR film. ND is the neutral density filter, and L_1 and L_2 are lenses.

Using the above setup, we studied the optical switching properties of the bR film at different pump and probe intensities. When the pumping intensity is too low (<0.56 mW/mm^2), no appreciable change in the transmitted probe beam intensity is observed (not shown here) regardless the probe beam intensity. This phenomenon is easy to understand. Since the pump beam is too weak, only few populations on each intermediate state can be transferred to other states by the pump beam; most of the populations keep staying on the same intermediate states as they do without the pump beam. Therefore, the transmitted probe beam intensity is unchanged.

#3422 - $15.00 US Received 2 December 2003; revised 26 February 2004; accepted 28 February 2004

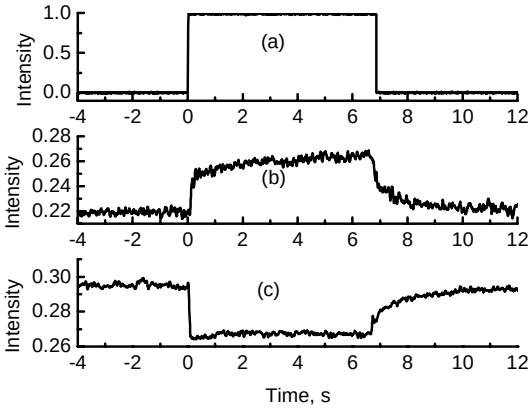

Fig. 4. (a) The normalized pump beam intensity at λ=532 nm, (b) and (c) are the transmitted probe beam intensity when the probe beam intensity is 3.1 mW/mm^2 and 310 mW/mm^2.

If the pump beam intensity is high enough, it can significantly change the transmitted probe beam intensity, functioning as an optical switch. The optical switching characteristics are very sensitive to the probing beam intensity as well as the pumping duration. In our experiments, we fixed the pumping beam (λ=532 nm) intensity at I=56 mW/mm^2. Figure 4(a) shows the normalized intensity of the pump beam. When the probe beam intensity is less than ~3.1 mW/mm^2, the illumination of the pump beam causes the transmitted probe beam to increase, as shown in Fig. 4(b). On the contrary, as the probe beam intensity is higher than ~310 mW/mm^2, the presence of the pump beam decreases the transmitted probe beam intensity, as shown in Fig. 4(c).

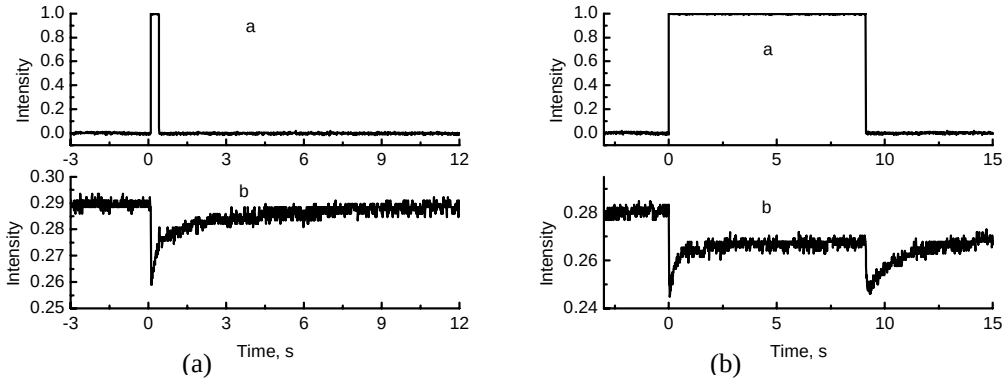

Fig. 5. Transient behavior of the probing beam under different pumping pulse width: (a) 0.3 s and (b) 8 s. Pumping beam (top; λ=532 nm) intensity I= 56 mW/mm^2 and probing beam (bottom trace; λ=633 nm) I=31 mW/mm^2.

As the probe intensity reaches ~31 mW/mm^2, an interesting phenomenon occurs, as shown in Fig. 5. Upon the illumination of the pump beam on the sample, the transmitted probe beam intensity drops quickly at the very beginning and then rises slowly. If the pumping duration is short enough, the transmitted intensity of the probing beam continues to rise back to the initial

#3422 - $15.00 US Received 2 December 2003; revised 26 February 2004; accepted 28 February 2004

value, as shown in Fig. 5(a). However, if the pump beam is kept on for a while, i.e. several seconds, the transmitted intensity of the probe beam slowly increases to a certain level, which depends on the intensity of the pump beam, and then remains unchanged till the pump beam is blocked. Once the pumping beam is blocked, the transmitted probe beam intensity quickly decreases again and then slowly increases to the initial value, as shown in Fig. 5(b).

The above phenomena cannot be simply explained by the two-state model. All the contributions from each intermediate state in bR's photocycle must be considered. Since the bR photocycle is very complicated, we have developed a theoretical model to look into the population distribution on each intermediate state.

3. Theoretical analysis

According to the bR's photocycle shown in Fig. 1, we propose a general energy level diagram shown in Fig. 6. Like the Br state, each intermediate state also contains its ground

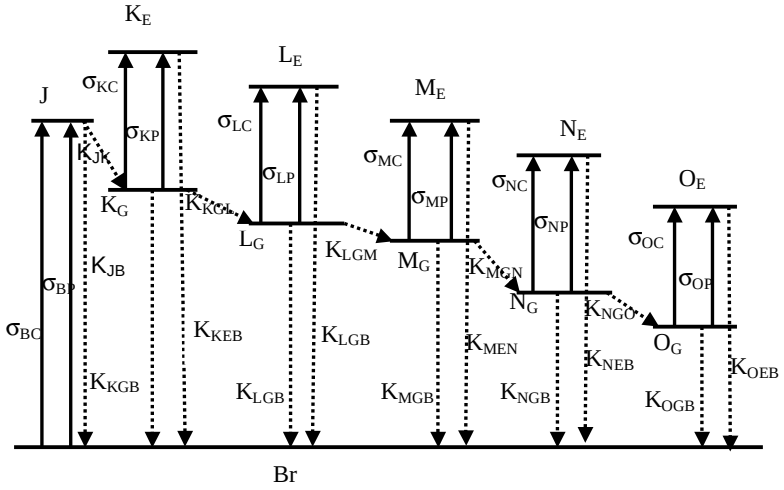

Fig. 6. Simplified level diagram representing the photocycle of bR molecules.

and excited states. In our experiment, the bR molecules were exposed to two laser beams with intensities I_C' and I_P'. We can describe the excitation and relaxation processes by the rate equations as follows:

$$\frac{dN_B}{dt} = -(\sigma_{BC} I_C + \sigma_{BP} I_P) N_B + K_{JB} N_J + \sum (K_{iGB} N_{iG} + K_{iEB} N_{iE}) \tag{1.a}$$

$$\frac{dN_J}{dt} = (\sigma_{BC} I_C + \sigma_{BP} I_P) N_B - (K_{JB} + K_{JK}) N_J \tag{1.b}$$

$$\frac{dN_{KG}}{dt} = K_{JK} N_J - (\sigma_{KC} I_C + \sigma_{KP} I_P + K_{KGB} + K_{KGL}) N_{KG} \tag{1.c}$$

$$\frac{dN_{KE}}{dt} = (\sigma_{KC} I_C + \sigma_{KP} I_P) N_{KG} - K_{KEB} N_{KE} \tag{1.d}$$

$$\frac{dN_{LG}}{dt} = K_{KGL} N_{KG} - (\sigma_{LC} I_C + \sigma_{LP} I_P + K_{LGB} + K_{LGM}) N_{LG} \tag{1.e}$$

#3422 - $15.00 US Received 2 December 2003; revised 26 February 2004; accepted 28 February 2004

$$\frac{dN_{LE}}{dt} = (\sigma_{LC} I_C + \sigma_{LP} I_P) N_{LG} - K_{LEB} N_{LE} \quad (1.f)$$

$$\frac{dN_{MG}}{dt} = K_{LGM} N_{LG} - (\sigma_{MC} I_C + \sigma_{MP} I_P + K_{MGB} + K_{MGN}) N_{MG} \quad (1.g)$$

$$\frac{dN_{ME}}{dt} = (\sigma_{MC} I_C + \sigma_{MP} I_P) N_{MG} - K_{MEB} N_{ME} \quad (1.h)$$

$$\frac{dN_{NG}}{dt} = K_{MGN} N_{MG} - (\sigma_{NC} I_C + \sigma_{NP} I_P + K_{NGB} + K_{NGO}) N_{NG} \quad (1.i)$$

$$\frac{dN_{NE}}{dt} = (\sigma_{NC} I_C + \sigma_{NP} I_P) N_{NG} - K_{NEB} N_{NE} \quad (1.j)$$

$$\frac{dN_{OG}}{dt} = K_{NGO} N_{NG} - (\sigma_{OC} I_C + \sigma_{OP} I_P + K_{OGB}) N_{OG} \quad (1.k)$$

$$\frac{dN_{OE}}{dt} = (\sigma_{OC} I_C + \sigma_{OP} I_P) N_{OG} - K_{OEB} N_{OE} \quad (1.l)$$

where $I_C = I_C^{'} / h\nu_C$ and $I_P = I_P^{'} / h\nu_P$ represent the photon density flux of the probe and pump beams, respectively. σ_{iC} and σ_{iP} (i = B, K, L, M ,N and O) are the absorption crosssection of the intermediate states at the probe and pump wavelength, respectively. N_{iG} and N_{iE} represent the population density on the ground and excited states of each intermediate state. The rate constant $K_{iGj} = 1/T_{iGj}$ represents the transition from the ground state of the i^{th} intermediate state to the ground state of the j^{th} intermediate state. The rate constant $K_{iEB} = 1/T_{iEB}$ represents the transition rate from the excited state of the i^{th} intermediate state to the Br state.

The variation of the probe beam intensity ($I_C^{'}$) with propagation depth z inside the bR film is governed by

$$\frac{dI_C^{'}}{dz} = -\alpha I_C^{'} \quad (2)$$

where

$$\alpha = N_B \sigma_{BC} + N_K \sigma_{KC} + N_L \sigma_{LC} + N_M \sigma_{MC} + N_N \sigma_{NC} + N_O \sigma_{OC} \quad (3)$$

Theoretically speaking, we can simulate the experimental results by numerically computing Eqs. (1) and (2). However, there are so many variables in Eq. (1) it is very difficult to choose a set of suitable parameters that could fit the experimental results exactly. Therefore, we try to use the model to qualitatively analyze the phenomena described above instead of accurately simulating the experimental results.

Since all the excited states involved have a relatively short lifetime, it is reasonable to assume that the rate constant from each excited state to Br is the same and large. Let us assume $K_{KEB} = K_{LEB} = K_{MEB} = K_{NEB} = K_{OEB} = 5\times10^7$ s^{-1}. Since the rate constant from each ground state to Br state K_{iGj} is very small, we can simplify the calculation by

#3422 - $15.00 US Received 2 December 2003; revised 26 February 2004; accepted 28 February 2004

assuming $K_{KGB} = K_{LGB} = K_{MGB} = K_{NGB} = K_{OGB} = 1\times10^{-3}$ s^{-1}. K_{JK} and K_{JB} are assumed to be 5×10^{7} and 1.67×10^{7} s^{-1}, respectively. The other parameters are listed in Table 1.

Table 1. The rate constants and absorption cross-sections used in our simulations.

Rate Constant	Value (s^{-1})	Absorption cross-section	Value (cm^2)	
			λ=532 nm	λ=633 nm
		σ_B	1.63×10^{-16}	0.6×10^{-16}
K_{KGL}	3.3×10^{4}	σ_K	1.06×10^{-16}	1.8×10^{-16}
K_{LGM}	2×10^{2}	σ_L	1.63×10^{-16}	0.02×10^{-16}
K_{MGN}	0.2	σ_M	0.38×10^{-16}	0.01×10^{-16}
K_{NGO}	50	σ_N	2.1×10^{-16}	0.2×10^{-16}
K_{OGB}	1	σ_O	0.7×10^{-16}	2.0×10^{-16}

Figure 7(a) shows the calculated variation in the normalized population density of each intermediate state when the probe beam intensity is 3.1 mW/mm^2. Before the pump beam is turned on, the majority of the populations are on the initial Br state. But due to the depletion of the populations of the initial Br state by the probe beam and the long lifetime of M and O states in comparison to K, L and N intermediate states, parts of the molecules are on M and O intermediate states and few molecules are on K, L, and N states. With the illumination of the green pumping beam, the populations of Br state dramatically decrease and the M-state populations dramatically increase. In addition, the O-state populations decrease while those of the L state increase slightly. However, there is no appreciable variation on the population of the K and N states. The reason is that λ=532 nm is close to the absorption peak of the Br state and most of the molecules are on Br state. A strong green laser beam can pump much more Br state populations to the excited state than those of all the intermediate states returning to the Br state. The excited molecules undergo K, L, M, N and O intermediate states and then finally go back to the initial Br state. Since M state has a much longer lifetime than the other intermediate states, most of the populations are accumulated in the M state. Due to the excitation and relaxation processes, the L-state populations increase a little while the O-state populations decrease slightly. The absorption cross-section of M and L states is less than that of Br and O states at λ=633 nm, which means a bR molecule on the M and L states can absorb less He-Ne laser light than it can on the O and Br states. Thus, the transmitted probing beam intensity increases as shown by the dashed lines in Fig. 7(a). After the pump beam is blocked, the molecules excited by the pump beam relax back to the initial Br state, causing the absorption to return to the initial value, as depicted in Fig. 7(a).

For the probe beam with a high intensity (>310 mW/mm^2), the situation is completely different, as shown in Fig. 7(b). Although the absorption cross-section of the Br state at λ=633 nm is small, the high intensity probing beam can still bleach the molecules from Br state. Again because of the long lifetime of M state, most of the molecules are accumulated on M state. Few molecules are on O state due to the high intensity and large absorption cross-section of O state at λ=633 nm. Therefore, before the illumination of the pump beam, most molecules are on M state, as shown in Fig. 7(b). The illumination of the green pump beam redistributes the populations of each state. At λ=532 nm, the absorption cross-section of Br state is larger than that of M state. However, since most of the molecules are on M state and few molecules are on Br state, the molecules transferred from M to Br state by the pump

#3422 - $15.00 US Received 2 December 2003; revised 26 February 2004; accepted 28 February 2004

beam exceed those relaxed back from Br to M state. As a result, the M-state populations decrease and Br-state populations increase. Since few spare molecules on Br

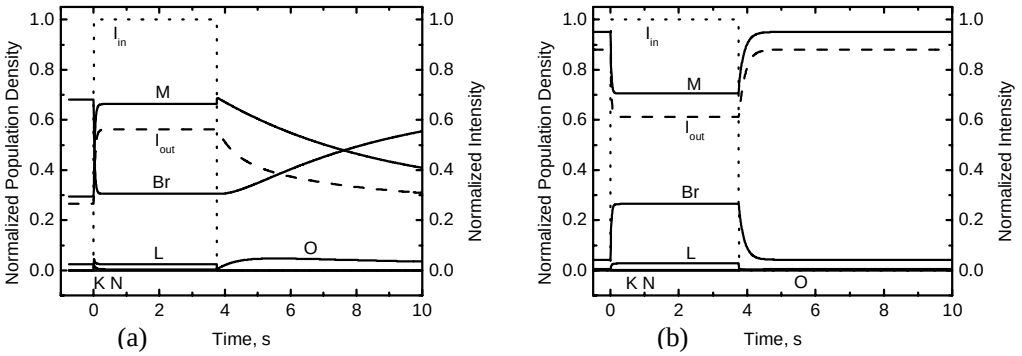

Fig. 7. Variation of the normalized population density of B, K, L, M, N and O states and the corresponding normalized transmitted intensity of the probe beam at λ=633 nm when the probe intensity is: (a) 3.1 mW/mm^2, (b) 310 mW/mm^2. The intensity of the pump beam at λ=532 nm is 56 mW/mm^2 (dashed line).

state are excited by the pump beam to go through the photocycle, there is no appreciable variation in the populations of the K, L, N and O states, as shown in Fig. 7(b). Again since the absorption cross-section of Br is larger than that of M at λ=633 nm, the transmitted probing beam intensity decreases as shown in the dashed lines in Fig. 7(b). After the green beam is blocked, the populations on Br state are bleached back to M state by the red beam and, therefore, the absorption increases to the initial value, as shown in Fig. 7(b).

As the intensity of the red probe beam reaches ~31 mW/mm^2, the status becomes very complicated. Before the illumination of the pump beam, most of the molecules have been excited to M state by the probe beam. In this case, a portion of molecules stay on O state because the probe beam intensity is not high enough to deplete all the O-state populations. When the pump beam is present, the populations of Br and L states are increased and those of

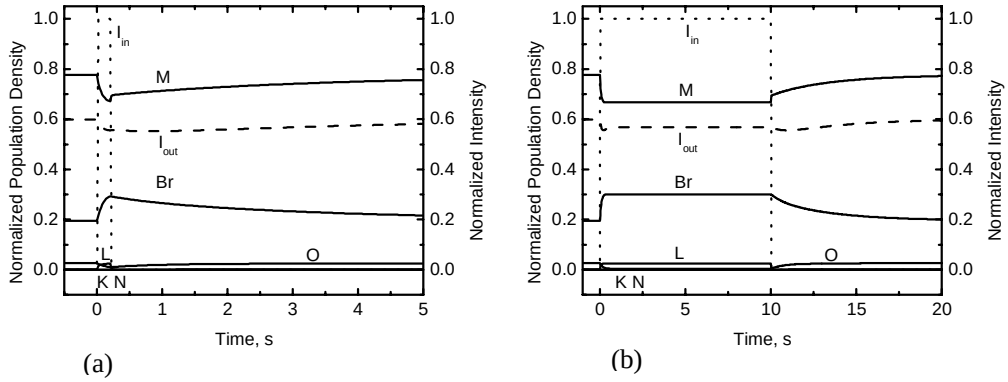

Fig. 8. Variation of the normalized population density of B, K, L, M, N and O states and the corresponding normalized transmitted intensity of the probe beam at λ=633 nm when the pump time is: (a) 0.3 s, (b) 8s. The intensity of the pumping beam at λ=532 nm is 56 mW/mm^2 (dashed line).

#3422 - $15.00 US Received 2 December 2003; revised 26 February 2004; accepted 28 February 2004

M and O states are decreased. If the pumping duration is too short, the populations of each intermediate state start to vary in the inverse direction before they reach a new dynamic balance under the illumination of both probe and pump beams. As a result, the transmitted probe beam intensity decreases first and then rises up to the initial value. When the pumping beam stays long enough, the populations of each state will reach a new dynamic balance. Since the population variation of L and O states are comparable to that of Br and M states, the contribution from L and O states is not negligible. The absorption cross-section of O state at λ=633 nm is larger than that of Br and M states so it largely affects the absorption properties. This is the main reason that the absorption quickly decreases and then rises slowly as the pump beam is switched on and off, as shown by the dashed line in Fig. 8 (b).

4. All-optical logic gates

Based on the optical switching properties at λ=633 nm, we have designed 11 kinds of variable binary all-optical logic gates using the bR film. The two incident λ=532 nm beams act as two inputs A and B and the transmitted He-Ne laser beam at λ=633 nm bears the output of the logic gate, as shown in Fig. 9.

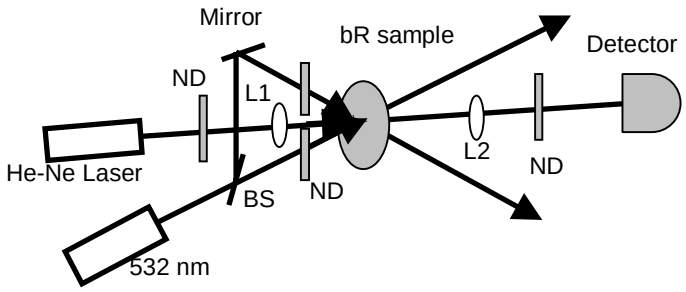

Fig. 9. Experimental setup for demonstrating an all-optical logic gate.

When the intensity of the two green beams is low (<0.56 mW/mm^2), there is no appreciable change in the transmitted probe beam intensity. This characteristic can be designed as the 0 or 1 logic gate by setting the threshold level above or below the transmitted probe intensity, respectively, as illustrated by the dashed line in Fig. 10(a) and Fig. 10(b).

When the pumping intensity is high (~56 mW/mm^2) and the probe intensity is low (<3.1 mW/mm^2), the transmitted probe beam intensity increases as one of the pumping beams is turned on, as shown in Fig. 4(b) and Fig. 7(a), and increases further when both pumping beams are simultaneously on. These switching characteristics shown in Figs. 11(a), (c) and (d) behave like the all-optical OR logic gate, since the output is high as long as one of the inputs is present and is low only when none of the inputs is present.

With the same configuration, an all-optical AND logic gate can be obtained by setting the threshold level as the dashed line shown in Fig. 11(b). In this case, the output is regarded as 0 when either one or none of the pump is present and 1 only when both the inputs are present simultaneously.

When one pump beam is less than 0.56 mW/mm^2 while the other one is ~56 mW/mm^2, the transmitted intensity of the probe beam increases only when the high intensity input beam is present. Figure 12 shows that this configuration functions as an A/B logic gate.

In the case that both pump (~56 mW/mm^2) and probe (~310 mW/mm^2) beams have high intensities, when the pump beam is on the transmitted probe beam intensity is reduced due to the increased absorption of Br state shown in Figs. 4(b) and 7(b). These switching characteristics can be used to design the all-optical NOR logic gate. In this case, the output is

#3422 - $15.00 US Received 2 December 2003; revised 26 February 2004; accepted 28 February 2004

low when either one or both the inputs are present and is high only when none of the pump beam is present, as shown in Fig. 13.

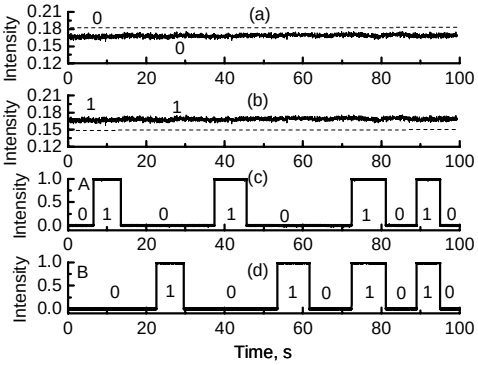

Fig. 10. All-optical logic gate: (a) optical 0 gate function, (b) optical 1 gate function (dashed line as the threshold level), both with unchanged normalized transmitted intensity of the probe beam at λ=633 nm as output with time; (c) and (d) are normalized profiles of the two inputs A and B. The intensity of the He-Ne probing beam is 3.1 mW/mm^2, and the intensity of the two inputs is 0.56 mW/mm^2.

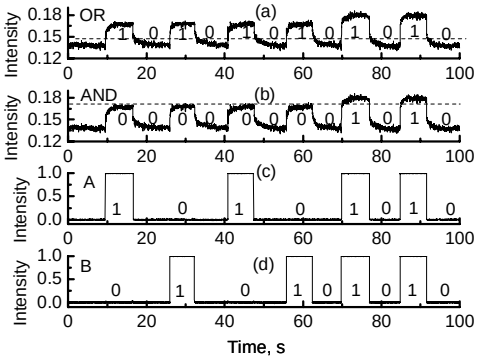

Fig. 11. All-optical logic gate: (a) optical OR gate function, (b) optical AND gate function (dashed line as the threshold level), both with variation of normalized transmitted intensity of the probe beam at λ=633 nm as output with time; (c) and (d) are normalized profiles of the two inputs A and B. The intensity of the He-Ne probing beam is 3.1 mW/mm^2, and the intensity of the two inputs is 56 mW/mm^2.

Using a low intensity (<0.56 mW/mm^2) and a high intensity (~56 mW/mm^2) pump beams as the inputs A and B, respectively, a $\overline{A}/\overline{B}$ logic gate can be obtained, as shown in Fig. 14. In this case, the output becomes 0 only when the input (A or B) with high intensity is present and 1 when the other one (B or A) with low intensity or none of them is present.

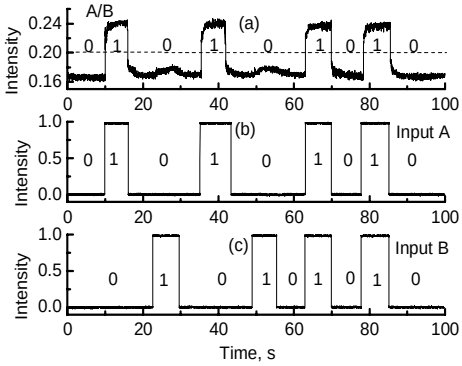

Fig. 12. All-optical logic gate: (a) optical A/B gate function (dashed line as the threshold level), (b) and (c) are normalized profiles of the two inputs A and B. The intensity of the He-Ne probing beam is 3.1mW/mm2, and the intensity of the inputs A and B is 0.56 mW/mm^2 and 56 mW/mm^2.

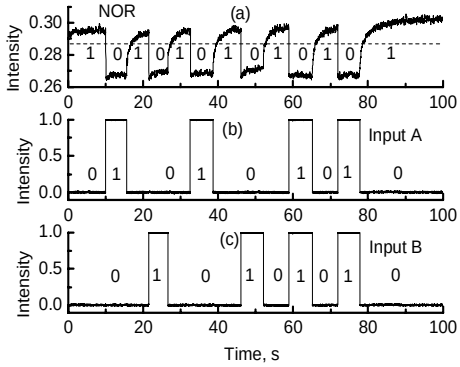

Fig. 13. All-optical logic gate: (a) optical NOR gate function (dashed line as the threshold level), both with variation of normalized transmitted intensity of the probe beam at 633 nm as output with time; (b) and (c) are normalized profiles of the two inputs A and B. The intensity of the He-Ne probing beam is 310 mW/mm^2, and the intensity of the two inputs is 56 mW/mm^2.

#3422 - $15.00 US Received 2 December 2003; revised 26 February 2004; accepted 28 February 2004

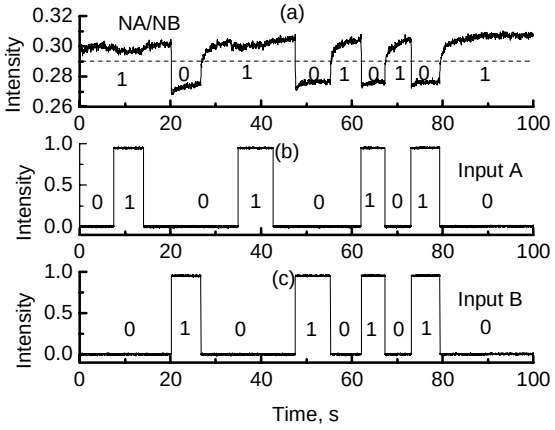

Fig. 14. All-optical logic gate: (a) optical NA/NB gate function (dashed line as the threshold level); (c) and (d) are normalized profiles of the two inputs A and B. The intensity of the He-Ne probing beam is 310 mW/mm^2, and the intensity of the inputs A and B is 0.56 mW/mm^2 and 56 mW/mm^2, respectively.

For the probe beam intensity is at ~31 mW/mm^2, the illumination of a short pulse pump beam induces a transient downward pulse in the transmitted probe intensity, as shown in Figs. 5(a) and 8(a). This characteristic corresponds to an inverted leading edge differentiator. However, if we set the threshold level as shown by the dashed line c1 in Fig. 15(a), a NOT

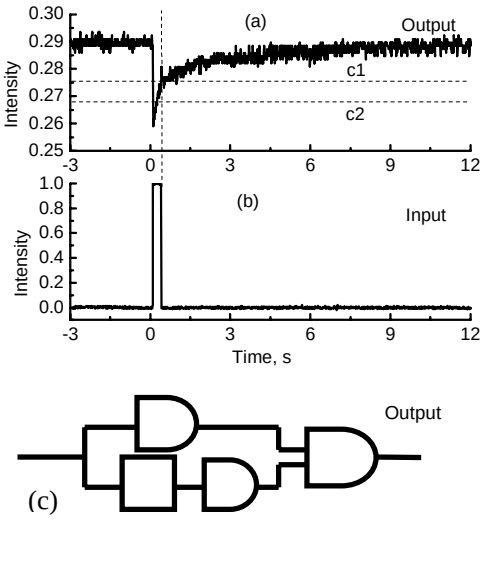

Fig.15. All-optical logic gate: (a) a combinational logic function as in (c) (dashed line as the threshold level); (b) is normalized profile of the input; (c) a combinational logic gate, T_L is a leading edge-triggered flip-flop, D is time-delay device. The intensity of the probing He-Ne laser beam is 31 mW/mm^2, and the intensity of the inputs is 56 mW/mm^2.

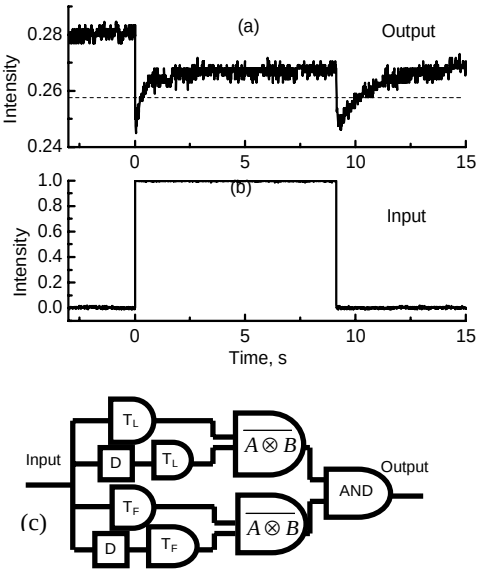

Fig.16. All-optical logic gate: (a) a combinational logic function as in (c) (dashed line as the threshold level); (b) is normalized profile of the input; (c) a combinational logic gate, T_L is a leading edge-triggered flip-flop, T_F is a falling edge-triggered flip-flop, D is time-delay device. The intensity of the probing beam is 31mW/mm^2, and the intensity of the inputs is 56 mW/mm^2

#3422 - $15.00 US Received 2 December 2003; revised 26 February 2004; accepted 28 February 2004

logic gate can be obtained. If we set the threshold level below line c1, i.e. as the dashed line c2 in Fig. 15(a), it functions as a combinational logic gate illustrated in Fig. 15(c). From Fig. 15(c), the input is divided into two routes. One goes through a leading edge-triggered flip-flop and the other goes through a time-delay and leading edge-triggered flip-flop. The outputs are the two inputs of $\overline{A \otimes B}$.

When the pump beam stays on for several seconds, the transmitted probing beam intensity quickly decreases at the very beginning and then slowly increases to a certain level when the pump beam is switched on and off, as shown in Figs. 5(b) and 8(b). If the threshold level is set as the dashed line in Fig. 16(a), the device functions as the combinational logic gate shown in Fig. 16(c). The input is divided into 4 routes: two of them go through a leading edge-triggered flip-flop, a time-delay and a leading edge-triggered flip-flop, and then are combined by a $\overline{A \otimes B}$ logic gate. The other two are combined by a $\overline{A \otimes B}$ logic gate after going through a falling edge-triggered flip-flop, and a time-delay and a falling edge-triggered flip-flop. Finally, the two outputs are combined by an AND logic gate.

5. Conclusion

We have experimentally investigated all-optical switching of bR film using green laser as pumping beams and red laser as probing beams. The switching characteristics have been qualitatively analyzed using a theoretical model including the six intermediate states in the photocycle. Based on the optical switching characteristics, we have designed and demonstrated 11 kinds of various binary logic gates with the same bR film by setting the pump and probe beams at suitable intensities. The proposed all-optical logic gates including 0, 1, AND, A/B OR, NOR, NA/NB, especially the last two logic gates would be useful for integrated optics due to the advantages of compact size, simple setup and design flexibility.

Acknowledgments

The authors are indebted to Haiying Wang for useful discussions and Janet Wu for proofreading the manuscript. The UCF group is supported by DARPA under Contract No. DAAD19-02-1-0208. The ECNU and Fudan groups are supported by the National Science Foundation of People's Republic of China under grant No.30100034.

#3422 - $15.00 US Received 2 December 2003; revised 26 February 2004; accepted 28 February 2004